Enhancement of the stability of fluorine atoms on defective graphene and at graphene/fluorographene interface

Enhancement of stability of fluorine atoms on defected graphene and at graphene/fluorographene interface

Zhimin Ao,[1*] Weichang Wu,[2] Shuang Li,[3] Hao Liu,[1] F. M. Peeters,[4] Sean Li,[2] Guoxiu Wang[1*]

1. Centre for Clean Energy Technology, School of Chemistry and Forensic Science, University of Technology Sydney, PO Box 123, Broadway, Sydney, NSW 2007, Australia
2. School of Materials Science and Engineering, The University of New South Wales, Sydney, NSW 2052, Australia
3. Nano Structural Materials Center, Nanjing University of Science and Technology, Nanjing 210094, Jiangsu, PR China
4. Department of Physics, University of Antwerp, Groenenborgerlaan 171, B-2020 Antwerpen, Belgium

Fluorinated graphene is one of the most important derivatives of graphene and has been found to have great potential in optoelectronic and photonic nanodevices. However, the stability of F atoms on fluorinated graphene under different conditions, which is essential to maintain the desired properties of fluorinated graphene, is still unclear. In this work, we investigate the diffusions of F atoms on pristine graphene, graphene with defects and at graphene/fluorographene interfaces by using density functional theory calculations. We find that an isolated F atom is not stable and diffuses easily on graphene, but the stability can be enhanced by inducing vacancies or absorbates in graphene and by creating graphene/ fluorographene interfaces, which would strengthen the binding energy of F atoms on graphene and increase the diffusion energy barrier of F atoms remarkably.

* Corresponding authors. Email: Zhimin.Ao@uts.edu.au (Z.A.), Guoxiu.Wang@uts.edu.au (G.W.)

In the past few years, covalently modified graphene derivatives prepared by attachment of hydrogen, halogens, or other atoms have attracted considerable interest to tune the properties of graphene for their potential applications[1], such as in nanoelectronic devices and as hydrogen storage materials. Besides graphene oxide and graphane, fluorographene—fully fluorinated graphene is another important structural derivative of graphene[1,2,3]. Fluorographene has a similar geometric structure and sp^3 bonding configuration as graphane, with each carbon covalently bonded to one fluorine atom. Fluorinated graphene is synthesized mainly by reacting graphene with XeF_2 and F_2[4,5] or with CHF_3 and CF_4 plasma[6,7], or by mechanical and chemical exfoliation of graphite fluoride[8,9]. The attachment of fluorine atoms to sp^2 carbons would significantly affect the electronic properties and local structure of the materials but preserves the 2D hexagonal symmetry. Such structural change would open the zero band gap of pristine graphene to ~3 eV[10]. Fluorographene is also found to have high transparency and fascinating insulating properties, which make it being the world's thinnest transparent insulator, and it has great potential in optoelectronic and photonic nanodevices[11,12].

First-principles studies on graphene monofluoride started in 1993[13], motivated by available experiments on graphite monofluoride. Theoretical calculation also predicts that partial fluorination of graphene from $C_{32}F$ to C_4F is able to tune the band gap from 0.8 to 2.9 eV [2,14,15]. As a result, through patterning graphene by selective fluorination of graphene sheet using a low-damage CF_4 plasma treatment, it can be achieved conductive (pristine graphene), semiconductive (partially fluorinated graphene) and insulator (highly fluorinated graphene) areas in the same graphene sheet [6]. Moreover, fluorination of selective areas of graphene can also been achieved by removing F atoms from fluorographene by electron beam[16] or by local deposition of F atoms through laser irradiation with fluoropolymers[17]. In addition, lateral graphene/fluorographene hybrid nanoribbons field-effect transistor has been found

experimentally to have very high ON-OFF switching ratio of 10^5 at room temperature. These devices also demonstrate excellent current-voltage saturation, providing a potential path for active radio-frequency application [18]. This hybrid graphene/fluorographene nanoribbons have also been studied by first-principles calculations to investigate the structural and electronic properties[10]. It is found that the electronic and magnetic properties of hybrid graphene/ fluorographene nanoribbons are tuneable depending on the interface type (armchair or zigzag interface), width of nanoribbons and terminations of the edge, which are promising for the realization of the graphene materials-based spintronics applications.

Although graphene fluoride and graphene/fluorographene hybrid nanoribbons have been found to have great potential for applications in optoelectronic and photonic nanodevices, the thermodynamic stability of F atoms on fluorinated graphene or at graphene/fluorographene interface is not clearly understood, which is essential to maintain the excellent properties of graphene fluoride and graphene/fluorographene heterostructure. It is known that the stability of H atoms at the interface of graphene/graphane nanoribbons can be enhanced significantly compared with an isolated H atom on pristine graphene from *ab initio* calculations[19,20], and it was predicted that graphene/graphane nanoribbons are stable down to the limit of a single carbon chain[19]. Therefore, it is expected that the stability of F atoms at the interface of graphene/fluorographene nanoribbons (GFNRs) would also been enhanced remarkably. In this work, the thermodynamic stability of F atoms on graphene and at the interface of GFNRs are studied by density functional theory (DFT) calculations through investigating the diffusion of F atoms on graphene and at the interface of GFNRs. Due to the unavoidable defects in graphene in experiments, the effects of defects, such as adsorbates and vacancies, on the stability of F atoms on graphene are also investigated. Stability enhancement mechanisms for F atoms on graphene are analysed through discussing the binding energy and the electron transfer between F atoms and graphene.

Results

The stability of a F atom on pristine graphene: Previously the stability of fluorinated graphene with different fluorination degree was mainly indicated by the binding energy and bond length of F-C bonds, and the corresponding electron transfer[3,15,21,22,23]. However, the mobility of F atoms on fluorinated graphene is unclear. Especially, it is desirable to be able to tune the mobility of F atoms on fluorinated graphene for different applications. Therefore, we focus on the investigation of the mobility of F atoms on fluorinated graphene and provide different methods to tune the diffusion energy barriers. To simplify the investigation, the diffusion of an isolated F atom on graphene is first investigated. Figure 1(a) shows the supercell of graphene in the calculation. A F atom is chemically adsorbed on the C atom at position I in Figure 1(a). For the F atom, there are three different possible diffusion pathways as shown in Figure 1(a): to the nearest C (path 1), to the second nearest position (path 2), and to the opposite position (path 3), respectively. The relaxed atomic structure with one F atom adsorbed on graphene is shown in Figure 1(a), where we can see that the F atom induces a structural deformation of graphene. The C atom binding with the F atom protrudes from the graphene plane due to the change of the bonding character from sp^2 to sp^3-like hybridization, similar to the case of hydrogenated graphene[24]. This also agrees with previous reported result[25]. The obtained binding energy of the F-C bond E_b is -1.92 eV with bond length $l_{F\text{-}C}$= 1.535 Å. It is reported that E_b and $l_{F\text{-}C}$ show strong dependence on the degree of graphene fluorination[15, 21], where E_b varies from -1.48 to -3.41 eV with corresponding $l_{F\text{-}C}$ from 1.383 to 1.572 Å. In this work, as shown in Figure 1 the fluorination degree is 1 F atom in 18 C atoms, the obtained E_b and $l_{F\text{-}C}$ are consistent with the reported results of -2.32 eV and 1.565 Å[15], ~2.0 eV and ~1.6 Å[21] with the similar fluorination degree. It is already known that the chemical adsorption of F atoms would alter the electronic and magnetic properties of graphene and open its bandgap[25,27]. We are not going to discuss the electronic and magnetic

properties of fluorinated graphene in this work, but focus on the thermodynamic stability of F atoms on graphene and at the graphene/fluorographene interface. Using linear synchronous transition/quadratic synchronous transit (LST/QST) and nudged elastic band (NEB) methods, all the three possible diffusion pathways of a F atom on pristine graphene as shown in Figure 1(a) are calculated and the results are shown in Table 1, where the diffusion barrier E_{bar} is the energy difference between transition state (TS) and initial structure (IS) before diffusion, and the diffusion energy E_R is the energy difference between the final structure (FS) after diffusion and the initial structure (IS) before diffusion. To better understand how to determine the diffusion energy barrier and diffusion energy, the detailed diffusion pathway of an isolated F atom on graphene along path 1 is taken as an example and shown in Figure 2 where the atomic structures of IS, TS and FS are also inserted. As shown in Figure 2, along the diffusion pathway there is a high energy state-TS, which has an energy of 0.41 eV higher than that of IS, *i.e.* the diffusion energy barrier is 0.41 eV. As one can see, at TS the F atom desorbs from the graphene and locates at the bridge site the C-C bond. From the results listed in Table 1, it is found that the diffusion barriers for the two possible pathways 1 and 2 are very close at ~0.40 eV, while it is much higher for the pathway 3 at 0.54 eV owing to the longer diffusion distance and the fact that more C atoms are involved in the diffusion. Note that there is no energy difference before and after diffusion for all three diffusion pathways, which is understandable because all the C atoms have the same potential energy. Therefore, the lowest energy barrier for an isolated F on graphene is ~0.40 eV, which is also consistent with the reported value of 0.36 eV for an F atom diffusing on a 2×2 graphene supercell.[21] In general it is considered that a surface reaction at ambient temperature occurs when the energy barrier is smaller than 0.91 eV[26]. In addition, the diffusion time at room temperature can be predicted by the equation[27],

$$\tau = \frac{1}{ve^{\left(\frac{-E_{bar}}{k_B T}\right)}} \quad (1)$$

where v is in order of 10^{12} Hz, k_B is the Boltzmann constant and T = 298.15 K. For the F atom diffusion on graphene, $\tau = 5.78 \times 10^{-6}$ s. Therefore, it is expected that the isolated F atom has high mobility on the graphene surface at room temperature.

The stability of a F atom on graphene with defects: Some defects, such as vacancies, are unavoidable in graphene. The diffusion of a F atom is expected to be different if there is a defect nearby due to the change of electron distribution near the defect. It was reported that the diffusion barrier of transition metal (TM) atoms on graphene increases substantially from 0.2-0.8 eV to 2.1-3.1 eV if the TM atoms are coupled to a vacancy[28], and the desorption of H atoms on N-doped graphene was found much easier if there is another H atom nearby[29]. Therefore, we investigate the diffusion behaviour of a F atom on graphene with another F atom or a vacancy nearby. If the first F atom is adsorbed at position IV in Figure 1(a), the second F atom has three possible adsorption positions in the same carbon ring, *i.e.* positions I-III, near the first F atom. The second F adsorbed at position V in a neighbour C ring is also considered for an example. All the four possible configurations are calculated and we find that the configuration with the second F atom adsorbed at position I has the lowest energy, indicating the favourite configuration for the two F atoms adsorbed on graphene. The corresponding structure is shown in Figure 1(b). Similar to the case of one F atom adsorbed on graphene, the two C atoms binding with the two F atoms would protrude from the graphene layer. The binding energy of the F-C bond is -2.73 eV and the bond length is 1.484 Å. Compared with the case of graphene with an isolated F atom E_b = -1.92 eV and $l_{F\text{-}C}$= 1.535 Å, the binding is much stronger with shorter bond length. This also agrees with the reported result that E_b becomes stronger when the fluorination degree increases[21].

To consider the effect of another F atom on the diffusion behaviour of the F atom on graphene, the diffusions for the second F atom from position I to positions II, III or V with another F atom at position IV are calculated, respectively. The three diffusions are indicated

as paths 1-3 in Figure 1(b). The calculated results are listed in Table 1. It is found that pathway 1 is preferred with the lowest diffusion energy barrier although the diffusion energy is high. The low energy barrier for pathway 1 can be understood through analysing the atomic charges of the atoms at the five positions I-V. Based on Hirshfeld method[30], it is known that the charges on the five C atoms at positions I-V are 0.094, 0.004, 0.041, 0.094, 0.018 *e*, respectively, while the charges on the two F atoms are the same -0.149 *e*. For the F diffusion along paths 1 and 2, main interactions come from the attractive interaction of positively charged C atoms and repulsive interaction of the other negatively charged F atom. During the F atom diffusion, the attractive interaction from the C atom at position II or III is similar due to the similar atom charges they have. However, the repulsive interaction from the other F at position IV is much stronger for the path 2 due to the much shorter distance between the two F atoms. Thus, the diffusion along path 1 is easier. For the F diffusion along path 3, the attractive interaction between the F atom and the C atom at position V is weaker due to the weakly charged C atom. Although the repulsive interaction between the two F atoms benefits this diffusion, this interaction is too weak to have obvious effect due to the long distance between the two F atoms. Therefore, the diffusion along path 1 has the lowest barrier 1.28 eV, which is still much higher than that of 0.40 eV for an isolated F atom diffusion on graphene. Therefore, the diffusion of one F atom on graphene would be more difficult if there is another F atom nearby, which would change the electronic distribution and strengthen the F-C bonds, thus enhancing the stability of the F atoms on graphene.

Figure 1(c) shows the relaxed structure of one F atom chemically adsorbed on graphene with a vacancy. We find that the F atom prefers to adsorb at the C atoms at the vacancy and its total energy is much lower than those of the other configurations after considering all the possible adsorption configurations. The F atom is found to be close to the centre of the vacancy, and the F-C bond tilts to the graphene surface in contrast to F adsorbed

on graphene without a vacancy. This is induced by the attractive interaction between the other two C atoms at the vacancy and the F atom. The binding energy of the F-C bond is -4.42 eV with bond length 1.350 Å. The obtained binding energy is much larger than -1.92 eV of the F-C bond on graphene without vacancy, and a shorter bond length is found in the vacancy system, which is similar to the case of TM atoms coupled with a vacancy in graphene[28]. To better understand the interactions of the F atom with the three C atoms at the vacancy, the atomic charge of the system are calculated through the Hirshfeld method[30]. The results show that the two C atoms at positions IV and V have the same positive charge of 0.0025 *e* due to the symmetry of the two atoms, and the charges of the F atom and the C atom at position I are -0.0686 and 0.0989 *e*, respectively. The two C atoms at positions II and VI have charge of -0.0098 *e*. Therefore, repulsive forces are present between the negatively charged F atom and the two C atoms at positions II and VI, while the F atom feels an attractive interaction with the two positively charged C atoms at positions IV and V. Under these electrostatic interactions, it is understandable that the F atom locates at nearly the centre of the vacancy.

To understand the effect of the vacancy on the diffusion of the F atom on graphene, three possible diffusion pathways are calculated as shown in Figure 1(c), and the results are listed in Table 1. It shows that the diffusion barriers are increased substantially for all the three pathways as compared to the case of graphene without vacancy. It is also found that the F atom prefers to diffuse among the three C atoms at the vacancy with a lower energy barrier of 1.67 eV and there is no energy difference before and after diffusion. For the diffusion to positions II and III, much higher energy barriers of 3.11 and 2.88 eV are obtained, respectively. Therefore, vacancies can enhance the thermodynamic stability of the F atom on graphene significantly, and can be considered to be active sites and anchors for adsorbates. Note that, different from other cases, the attractive interactions between the two C atoms at

positions IV and V and the F atom also contribute to the binding energy of the C-F bond when determined through Equation (2) in the method section below. Therefore, the diffusion barrier among the three C atoms at the vacancy is relatively lower due to the fact that only part of the C-F interaction needs to be broken for this type of diffusion.

The stability of F atoms at the interface of graphene/fluorographene: It is known from the above discussion that the diffusion behaviour of one F atom would be different if there is another F atom nearby. Therefore, it is expected that the diffusion behaviour of one F atom at the interface of graphene/fluorographene nanoribbons would change remarkably due to the presence of more than one F atom in its neighbourhood. As shown in Figure 3, there are two types of interfaces: zigzag [Figure 3(a)] and armchair [Figure 3(b)] interfaces. For the both types of nanoribbons, the C atoms protrude from the C layer due to the bonded F atoms, which changes the C atoms into sp^3-like binding. In addition, for the zigzag GFNRs, both the graphene and fluorographene nanoribbons are flat [see Figure 3(a)]. However, the graphene and fluorographene layers are not in the same plane, and there is a tilt angle of about 150° at the interface, which is consistent with previous reported result[10]. For the armchair GFNRs [Figure 3(b)], the graphene and fluorographene regions are flat and in the same plane, which also agrees with Ref. [10]. The interfaces between graphene and fluorographene nanoribbons are the interfaces between sp^2 and sp^3 bonded C atoms. C atoms in graphene have sp^2 hybridization and the structure stabilizes as a flat sheet. The hybridization changes from sp^2 to sp^3 in fluorographenen due to the presence of alternating F atoms placed on both sides of the carbon plane. The sp^3 hybridization also forces nearest neighbour C atoms in fluorographene to lie in different planes. As shown in Figure 3(a), the closed C atoms in fluorographene at the right side of the zigzag interface are only bonded with F atoms below the fluorographene layer, which would push down the graphene nanoribbon due to the sp^3 hybridized C atoms. At the left side interface, the closed C atoms in fluorographene are only

bonded with F atoms above the fluorographene layer, which would push up the graphene nanoribbon due to the sp^3 hybridized C atoms. This induces a tilt angle of ~150° at the zigzag interface. For the armchair interface, the closed C atoms at both sides of the interface bind with F atoms above and below the fluorographene layer alternatively as shown in Figure 3(b). The pushing down and up forces at the interface are neutralized. Thus, the armchair graphene/fluorographene nanoribbons are flat without a tilt angle.

The stability of the two types of interfaces are analysed by calculating the diffusion barriers of the F atoms at the interfaces. For the case of a zigzag interface, there are two different types of C and F atoms, which are indicated as sites I and II in Figure 3(a). For the diffusion of the F atom at site I, there are three possible diffusion paths labelled as 1-3. For the F atom at site II, there are two possible diffusion pathways that we label as 4 and 5. In the case of an armchair interface, all the C atoms at the interface are equivalent from a diffusion point of view and there are five different diffusion pathways that we label as 6-10 in Figure 3(b). The diffusion barriers and diffusion energies for the different paths and for both types of graphene/fluorographene interfaces are summarized in Table 1. For the zigzag interface, it is found that the barriers are 1.92, 2.10, 2.40, 2.70, 2.68 eV for the pathways 1-5, respectively. Thus, the minimum diffusion barrier for the zigzag GFNRs is the F atom at site I diffusing to its nearest C atom along the C-C bond with an energy barrier of 1.92 eV. For the armchair interface, the energy barriers for pathways 6-10 are 2.26, 2.28, 2.28, 2.26, and 2.27 eV, respectively. Thus, the energy barrier for F diffusion at the armchair interface can be minimized to 2.26 eV to the second nearest C atom along path 6. For both zigzag and armchair interfaces, the minimum diffusion barriers of the F atoms are about 5 times larger than that of F diffusion on pristine graphene. In addition, the energy barriers for the F atom diffusion along the different paths at the armchair interface are almost the same ~2.26 eV, which is larger than the minimum diffusion barrier of F atoms at the zigzag interface. From

Table 1, we notice that all the F diffusion processes at the interfaces imply an increase of a couple of electronic volts in energy of the system after diffusion, which indicates that after the diffusion the energy needed for recovering the system back to the initial perfect thermodynamics state is always lower than the energy needed for distorting the interfaces. Therefore, the graphene/fluorographene interfaces are rather stable for both types of hybrid nanoribbons.

Discussion

The stability enhancement can be understood by calculating the binding energy of the F atoms in the different situations, which are proportional to the strength of the C-F bonds. It was reported that the diffusion barrier for an isolated H atom on graphene is ~0.3 eV, which was obtained by a DFT calculation using a similar method to this work[31]. The higher diffusion barrier here for an isolated F atom on graphene is due to the stronger binding energy of the C-F bond (-1.92 eV) than that of C-H (-0.88 eV) [20]. For the F atoms in other systems, E_b in graphene with a vacancy is enhanced to -4.42 eV with l_{C-F} = 1.350 Å, and the E_b for the two F graphene system is -2.73 eV with l_{C-F} = 1.484 Å. For the F atoms at the GFNRs interfaces, the binding energy of the C-F bond at sites I and II at the zigzag interface are -3.39 and -3.85 eV, respectively. The corresponding bond lengths are 1.400 and 1.395 Å. For the armchair interface of GFNRs, the bind energy at site III is -3.05 eV with bond length of 1.405 Å. This indicates a stability enhancement of the F atoms on graphene with defects and at the graphene/fluorographene interfaces due to the presence of stronger C-F bonds. The results of the binding energy and bond length also explain the stability order: F at the vacancy (E_b = -4.42 eV, l_{C-F} = 1.350 Å) > F at site II of zigzag interface (E_b = -3.85 eV, l_{C-F} = 1.395 Å) > F at site I of zigzag interface (E_b = -3.39 eV, l_{C-F} = 1.400 Å) > F at site III of armchair interface (E_b = -3.05, l_{C-F} = 1.405 Å) > F with another F atom nearby on graphene (E_b = 2.73 eV, l_{C-F} =

1.484 Å) > F on pristine graphene (E_b = -1.92 eV, $l_{C\text{-}F}$ = 1.535 Å). Note that the abnormal diffusion barrier of 1.67 eV for diffusion of a F atom at the vacancy along path 3 in Figure 1(c) is because only part of the C-F interaction is broken as discussed above, the actual minimum diffusion barrier is 2.88 eV, for diffusion along path 2. In addition, the energy barriers for the F atom diffusion along the different paths at the armchair interface are almost the same ~2.26 eV, while those for 5 diffusion paths at the zigzag interface are different. The different energy barriers at the zigzag interface are induced by the different binding energy of F-C bonds at sites I and II, and the tilt angle between fluorographene and graphene nanoribbons. The barriers for the diffusions from the site I along outside of the angle are always lower than those for the diffusions from the site II along inside of the angle. In order to have more clear ideal on the enhanced stability of F atoms on graphene with defects and at the interfaces of GFNRs, the corresponding diffusion times are predicted using Equation (1), and they are 4.33×10^{9}, 4.83×10^{36}, 2.85×10^{20} and 1.60×10^{26} s for F atoms on graphene with another F atoms, or with a vacancy, and at the zigzag and armchair interfaces of GFNRs, respectively. From the diffusion time, we can see the huge difference of the mobility of F atoms at the different conditions.

In conclusion, the diffusion of a single F atom on pristine graphene, graphene with another F atom adsorbed, graphene with a vacancy, and at graphene/fluorographene nanoribbons interfaces are investigated by DFT calculations. It is found that an isolated F atom diffuses easily on pristine graphene surface with a low energy barrier of about 0.40 eV with predicted diffusion time of 5.78×10^{-6} s, while inducing defects in graphene, such as adsorbate or vacancy, can increase the energy barrier significantly, thus preventing the diffusion of F atoms and enhancing the stability of F atoms on graphene remarkably. On the other hand, the energy barrier for F atoms at both zigzag and armchair interfaces increases by about a factor 5 as compared to an isolated F on graphene, indicating that F atoms are stable

at the interfaces. The enhancement mechanism is believed to originate from the stronger C-F bonds under those conditions. Therefore, the stability of F atoms on graphene can be tuned through different techniques, such as inducing defects in graphene and creating graphene/fluorographene interfaces, with diffusion time from 10^9 to 10^{36} s in order to maintain the excellent properties of fluorographene for applications in optoelectronic and photonic nanodevices.

Methods

The spin-polarised DFT calculations were executed using the DMOL^3 code. The generalized gradient approximation (GGA) with PBE functional was utilized as the exchange-correlation functional. A double numerical plus polarization (DNP) was used as the basis set, while the DFT semicore pseudopotentials (DSPP) core treatment was utilized to include relativistic effects. Spin polarization was included in the calculations. The convergence tolerance of the energy was set to 10^{-5} Ha (1 Ha=27.21 eV), and the maximum allowed force and displacement were 0.02 Ha and 0.005 Å, respectively. To inspect the diffusion pathways of fluorine atoms at the graphene surface, LST/QST and NEB tools in the DMOL^3 code were employed. The k-point is set as 12×12×1 to search for the structure of the transition state (TS) and the minimum energy pathway. In the simulations, 18 Å vacuum over the graphene layer is taken to minimize the interlayer interactions, three dimensional periodic boundary conditions were imposed, and all the atoms are allowed to relax. The DFT+D method within the Grimme scheme is used in all calculations to consider the van der Waals forces.[32] The binding energy (E_b) of a F-C bond can be determined by

$$E_b = E_i - (E_{i\text{-}F} + E_F) \quad (2)$$

where E_i is the total energy of the initial system, $E_{i\text{-}F}$ is the total energy of the initial system after deleting one F atom, and E_F is the energy of an isolated F atom.

References

1. Tang, Q., Zhen, Z. & Chen, Z. Graphene-related nanomaterials: tuning properties by functionalization. *Nanoscale* **5**, 4541-4583 (2013).
2. Leenaerts, O., Peelaers, H., Hernández-Nieves, A. D., Partoens, B. & Peeters F. M. First-principles inverstigation of graphene fluoride and graphane. *Phys. Rev. B* **82**, 195436 (2010).
3. Han, S. S. et al. Unraveling Structural Models of Graphite Fluorides by Density Functional Theory Calculations. *Chem. Mater.* **22**, 2142-2154 (2010).
4. Nair., R. R. et al. Fluorographene: A Two-Dimenionsional Counterpart of Teflon. *Small* **6**, 2877-2884 (2010).
5. Cheng, S.-H. et al. J. Reversible fluorination of graphene: Evidence of a Two-dimensional Wide Bandgap Semicondcutor. *Phys. Rev. B* **81**, 205435 (2010).
6. Ho, K.-I. et al. One-step Formation of a Single Atomic-layer Transistor by the Selective Fluorination of a Graphene Film. *Small* **10**, 989-997 (2014).
7. Chen, M. et al. Layer-dependent Fluorination and Doping of Graphene via Plasma Treatment. *Nanotechnology* **23**, 115706 (2012).
8. Zbořil, R. et al. Graphene Fluoride: A Stable Stoichiometric Graphene Derivative and its Chemical Conversion to Graphene. *Small* **6**, 2885-2891 (2010).
9. Chang, H. et al. Facile Synthesis of Wide-Bandgap Fluorinated Graphene Semiconductors. *Chem.-Eur. J.* **17**, 8896-8903 (2011).
10. Tang, S. & Zhang, S. Structural and Electronic Properties of Hybrid Fluorographene-Graphene Nanoribbons: Insight from First-Principles Calculations. *J. Phys. Chem. C* **115**, 16644-16651 (2011).
11. Zhu, M. et al. Fluorographene nanosheets with broad solvent dispersibility and their applications as a modified layer in organic field-effect transistors. *Phys. Chem. Chem. Phys.* **15**, 20992-21000 (2013).
12. Jeon, K.-J. et al. Fluorographene: A Wide Bandgap Semicondutor with Ultraviolet Luminescence. *ACS Nano* **5**, 1042-1046 (2011).
13. Charlier, J. -C., Gonze, X. & Michenaud, J. -P. First-principles study of graphite monofluoride $(CF)_n$. *Phys. Rev. B* **47**, 16162 (1993).
14. Robinson, J. T. et al. Properties of Fluorinated Graphene Films. *Nano Lett.* **10**, 3001-3005 (2010).
15. Liu, H. Y., Hou, Z. F., Hu, C. H., Yang, Y. & Zhu, Z. Z. Electronic and Magnetic Properties of Fluorinated Graphene with Different Coverage of Fluorine. *J. Phys. Chem. C* **116**, 18193-18201 (2012).
16. Withers, F., Bointon, T. H., Dubois, M., Russo, S. & Craciun, M. F. Nanopatterning of Fluorinated Graphene by Electron Beam Irradiation. *Nano Lett.* **11**, 3912-3916 (2011).
17. Lee, W. H. et al. Selective-Area Fluorination of Graphene with Fluoropolymer and Laser Irradiation. *Nano Lett.* **12**, 2374-2378 (2012).
18. Moon, S. S. et al. Lateral Graphene Heterostructure Field-Effect Transistor. *IEEE Elec. Dev. Lett.* **34**, 1190-1192 (2013).
19. Tozzini, V. & Pellegrini, V. Electronic Stucture and Peierls Instability in Graphene Nanoribbons Sculpted in Graphane. *Phys. Rev. B* **81**, 113404 (2010).
20. Ao, Z. M., Hernández-Nieves, A. D., Peeters, F. M.& Li, S. Enhanced Stability of Hydrogen Atoms at the Graphene/graphane Interface of Nanoribbons. *Appl. Phys. Lett.* **97**, 233109 (2010).
21. Santos, H. & Henrard, L. Fluorine Adsorption on Single and Bilayer Graphene: Role of Sublattice and Layer Decoupling. *J. Phys. Chem. C* **118**, 27074-27080 (2014).
22. Medeiros, P. V. C., Mascarenhas, A. J. S., de Brito Mota, F. & de Castilho, C. M. C. A DFT Study of Halogen Atoms Adsorbed on Graphene Layers. *Nanotechnology* **21**, 485701 (2010).

23. Wu, B. -R. & Yang, C.-K. Electronic Structures of Graphene with Vacancies and Graphene Adsorbed with Fluorine Atoms. *AIP Adv.* **2**, 012173 (2012).
24. Sofo, J. O. et al. *Phys. Rev. B* **83**, 081411 (2011).
25. Kim, H. -J. & Cho, J. -H. Fluorine-induced Local Magnetic Moment in Graphene: A Hybrid DFT Study. *Phys. Rev. B* **87**, 174435 (2013).
26. Young, D. C. *Computational Chemistry: A Practical Guide for Applying Techniques to Real World Problems.* (Wiley, New York, 2002).
27. Jiang, Q. G., Ao, Z. M., Li, S. & Wen, Z. Density Functional Theory Calculations on the CO Catalytic Oxidation on Al-embeded Graphene. *RSC Adv.* **4**, 20290 (2014).
28. Krasheninnikov, A. V., Lehtinen, P. O., Foster, A. S., Pyykkö, P. & Nieminen, R. M. Embedding Transition-Metal Atoms in Graphene: Structure, Bonding, and Magnetism. *Phys. Rev. Lett.* **102**, 126807 (2009).
29. Ao, Z. M., Hernández-Nieves, A. D., Peeters, F. M. & Li, S. The Electric Field as a Novel Switch for Uptake/release of Hydrogen for Storage in Nitrogen Doped Graphene. *Phys. Chem. Chem. Phys.* **14**, 1463-1467 (2012).
30. Hirshfeld, F. L. Bonded-atom Fragments for Describing Molecular Charge Densities. *Theor. Chim. Acta* **44**, 129-138 (1977).
31. Boukhvalov, D. W. Modeling of Hydrogen and Hydroxyl Group Migration on Graphene. *Phys. Chem. Chem. Phys.* **12**, 15367-71 (2010).
32. Grimme, S. Semiempirical GGA-type Density Functional Constructed with a Long-range Dispersion Correction. *J. Comput. Chem.* **27**, 1787-99 (2006).

Acknowledgements

We acknowledge the financial supports from the Chancellor's Research Fellowship Program of the University of Technology Sydney, the Flemish Science Foundation (FWO-Vl) and the Methusalem foundation of the Flemish Government. This research was also supported by the National Computational Infrastructure (NCI) through the merit allocation scheme and used NCI resources and facilities in Canberra, Australia.

Author contributions

Z. A. conceived the research, carried out calculations, analysed the simulation data and wrote the paper; W.W., Shuang Li, H.L., F. P., Sean Li and G.W. participated in the discussion and revised the manuscript. F. P., Sean Li and G.W. supervised and directed the project.

Additional information

Competing financial interests: The authors declare no competing financial interests.

Table 1| Diffusion barriers (E_{TS}-E_{IS}) for several diffusion paths (see Figures 1 and 3) and diffusion energy (E_{FS}-E_{IS}) for F atom diffusion at different conditions.

	Diffusion pathways	Diffusion energy (eV)	Diffusion barrier (eV)
One F atom on graphene	1	0	0.41
	2	0	0.40
	3	0	0.54
Two F atoms on graphene	1	1.12	1.28
	2	0.30	1.45
	3	0.78	1.37
One F atom on graphene with vacancy	1	2.85	3.11
	2	1.80	2.88
	3	0	1.67
Zigzag GFNR interface	1	1.27	1.92
	2	1.27	2.10
	3	1.01	2.40
	4	1.47	2.70
	5	1.50	2.68
Armchair GFNR interface	6	1.28	2.26
	7	2.00	2.28
	8	1.14	2.28
	9	2.09	2.26
	10	2.34	2.27

Figure captions

Figure 1 | Supercell of graphene used in the calculations. (a) One F atom on pristine grapehen, (b) two F atoms on pristine graphene, and (c) one F atom on graphene with a vacancy. In this and following figures, the arrows indicate the different diffusion pathways considered. The grey and blue balls are C and F atoms, respectively.

Figure 2 | The diffusion pathway of an isolated F atom on pristine graphene along path 1. The diffusion energy barrier is the energy difference between TS and IS, while the diffusion energy is the energy difference between FS and IS. The energy of IS is set to be 0.

Figure 3 | Atomic structure of graphene/fluorographene nanoribbons. (a) Zigzag and (b) armchair interfaces after geometry relaxation.

Figure 1

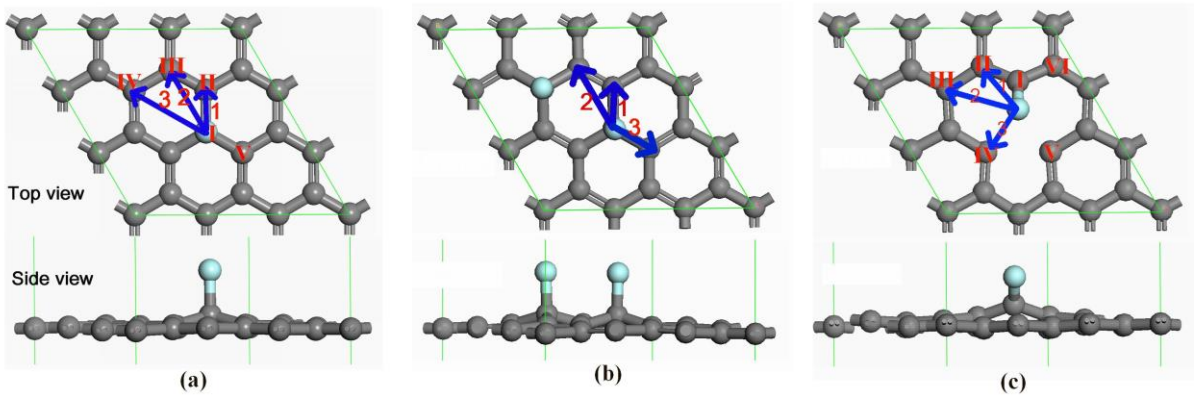

Figure 2

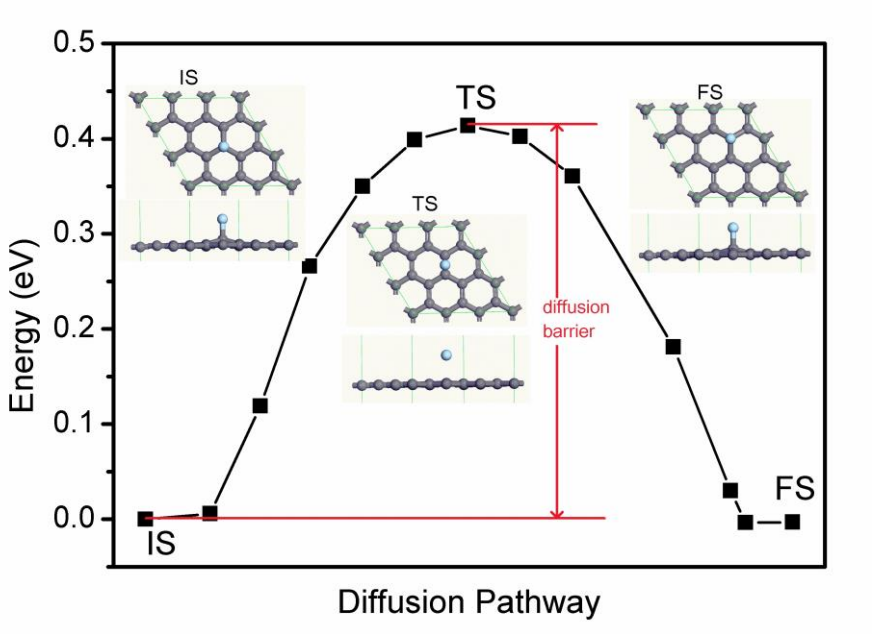

Figure 3